

# THREE ABUTMENT SCOUR CONDITIONS INVESTIGATED WITH LABORATORY FLUMES

Robert ETTEMA<sup>1</sup>, Tatsuaki NAKATO<sup>2</sup>, Atsuhiko YOROZUYA<sup>3</sup>, and Marian MUSTE<sup>4</sup>,

<sup>1</sup>Member of the ASCE, Professor, Dept. of Civil Eng., The Univ. of Wyoming  
(1000 E. University Street, Laramie, Wyoming 82071, U.S.A.)  
E-mail: ettema@uwyo.edu

<sup>2</sup>Member of the ASCE, Retired, IIHR – Hydrosience & Engineering, The Univ. of Iowa  
(618 Pine Ridge Road, Coralville, Iowa 52241, U.S.A.)  
E-mail: mollusk007@gmail.com

<sup>3</sup>Member of the JSCE, formerly Graduate Research Assistant, IIHR – Hydrosience & Engineering, The Univ. of Iowa

<sup>4</sup>Member of the ASCE, Research Engineer, IIHR – Hydrosience & Engineering, The Univ. of Iowa  
(100 SHL, IIHR – Hydrosience & Engineering, The Univ. of Iowa, Iowa City, Iowa 52242, U.S.A.)  
E-mail: marian-muste@uiowa.edu

Two practical new methods for estimating scour depths at abutments were developed based on extensive laboratory tests investigating three basic scour conditions at bridge abutments on floodplains. One new approach for scour-depth approach discards the old notion of linearly combining bridge-waterway constriction scour and local scour at the abutment structure. The method entails estimating an abutment-induced local amplification of contraction scour at the bridge opening, and separately estimating a maximum local scour depth at the abutment when exposed by highway embankment failure. The second approach entails determining the geotechnical stability limit for an embankment associated with an abutment, and then evaluating the scour depth likely to cause embankment failure at the abutment column.

A realistic abutment feature comprising a pile-supported structure set amidst erodible, earthfill approach embankment was considered in the investigation. This approach is the first major effort to consider abutment construction and to evaluate how it affects abutment scour processes. It has been found that abutment scour is as much a problem of embankment geotechnical stability as of hydraulic erosion of the channel bed or floodplain upon which the abutment and its embankment are placed.

Laboratory experiments were conducted with realistic abutments with approach embankments configured in a range of erodibility conditions, including fixed embankment on fixed floodplain, riprap-protected erodible embankment on readily erodible floodplain, and unprotected readily erodible embankment on readily erodible floodplain.

**Key Words:** *bridge abutment, abutment scour, embankment, contraction scour, compound channels*

## 1. INTRODUCTION

Though bridge abutment scour is an extensively studied topic, the prevailing perception among many hydraulic engineers is that the existing design relationships derived almost exclusively from laboratory flume experiments substantially over-predict scour depths. Scour depths observed at actual abutments typically are much smaller than those predicted. This paper presents new insight about the scour processes, and recommends two new approaches for estimating maximum depth of scour

at two common forms and construction layouts of abutment – spill-through and wing-wall abutments in compound channels. These abutment types, shown in Fig. 1, are very common in the U.S.A., and usually are located in floodplains.

The first approach is from the standpoint of flow hydraulics, and treats flow around an abutment as flow around a short construction, such that:

$$\text{abutment scour} = \text{short-contraction scour} \\ = (\text{coefficient}) \times (\text{long-contraction scour}) \quad (1)$$

This method is not entirely new. It was first suggested by Laursen (1960)<sup>1</sup>, and has been partially

developed in Chang and Davis (1998)<sup>2</sup>. Short-contraction scour is an amplification of long-contraction scour, as illustrated in Fig 2. The scour amplification occurs near the abutment, and is attributable to nonuniform distribution of flow around an abutment, and to large-scale turbulence structures generated by passing around the abutment. The term “*coefficient*” empirically takes into account the amplifying erosive effects on scour depth of nonuniform distribution of flow and of large-scale turbulence.

The second approach is from the geotechnical standpoint, and directly relates maximum scour depth to the geotechnical stability of the earthfill embankment at an abutment. It is possible to formulate the geotechnical limit to maximum scour depth. Fig. 3 illustrates this limit. As found in the flume experiments, the location of deepest scour,  $d_{S-MAX}$ , was a radial distance,  $R$ , out from the abutment column. For the present study (and many abutment embankments), the constructed embankment slope was 2 horizontal to 1 vertical, such that the requirement for embankment slope stability is met, when the slope extends back to the abutment column. The limiting scour depth can be estimated as

$$d_{S-MAX} = 4 \left( \frac{L}{Y_f} \right)^{0.2} Y_f \tan \theta_s - E_H \quad (2)$$



(a)



(b)

Fig. 1 Typical spill-through (a), and wing-wall (b) abutments

Fig. 3 indicates the terms in Eq. (2);  $\theta_s$  is the limiting value of slope angle for embankment stability. Once the embankment fails so as to expose

the abutment column, flow velocities reduce and the embankment may breach. Thereafter, scour does not deepen. Eq. (1) is introduced here, but not further discussed. This paper delves deeper in the hydraulics approach.

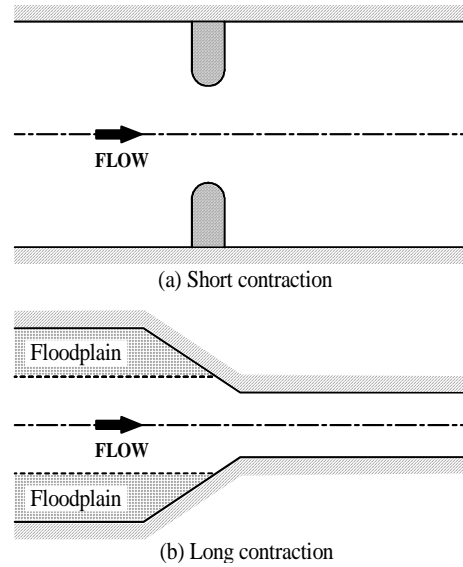


Fig. 2 Definition sketch of the short and long contractions

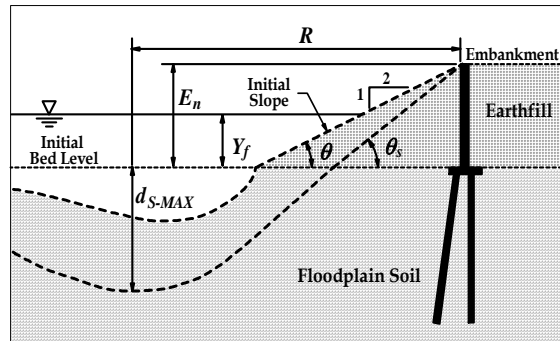


Fig. 3 Maximum scour depth is limited by embankment geotechnical stability (spill-through abutment)

## 2. THREE SCOUR CONDITIONS

### (1) Introduction

On the basis of the relative erodibility of sediments forming the main-channel bed, soils forming the floodplain, and the shear strength of the compacted earthfill approach embankment, three distinctive scour conditions of abutment scour were developed in response to the flow field at an abutment.

### (2) Scour conditions

Several abutment scour conditions develop in accordance with the flow field at an abutment, the physical characteristics of an abutment, and the

waterway where the abutment is located:

- (a) **Scour Condition A:** Scour of the main-channel bed when the floodplain is far less erodible than the bed of the main channel. Hydraulic scour of the main-channel bed causes the bank to become geotechnically unstable and collapse. The collapsing bank undercuts the abutment embankment, which in turn collapses locally. Soil, and possibly riprap, from the collapsed bank and embankment slide into the scour hole, as sketched in Fig. 4a.
- (b) **Scour Condition B:** Scour of the floodplain around the abutment. This scour condition is equivalent to scour at abutment placed in a rectangular channel. Because the sediment-transport rate on a floodplain is quite low, this scour condition usually occurs as clear-water scour. The scour hole locally destabilizes the embankment side slope, causing embankment soil, and possibly riprap to slide into the scour hole, as illustrated in Fig. 4b.
- (c) **Scour Condition C:** Scour Conditions A and B may eventually cause the approach embankment to breach near the abutment, thereby fully exposing the abutment column. For this condition, scour at the exposed stub column essentially progresses as if the abutment column were a pier, as illustrated in Fig. 4c. This scour condition usually occurs as clear-water scour.

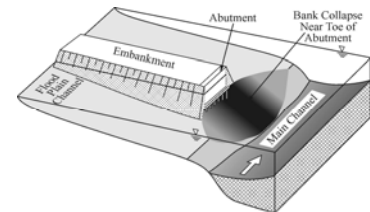
### 3. SHORT CONTRACTION SCOUR

The approach to scour-depth estimation undertaken here estimates the potential maximum depth of scour that may develop without immediately considering the geotechnical failure of the embankment on floodplain soil. For the purpose of design estimation of scour depth, it is necessary to consider the absolute depth elevations attained with the scour depths associated with Scour Conditions A through C. The essential notion underlying our estimation approach is that the potential maximum flow depth near an abutment can be expressed in terms of an amplified contraction scour estimated in terms of unit-discharge values for flow around an abutment. The maximum scour depth,  $Y_{MAX}$ , is estimated as

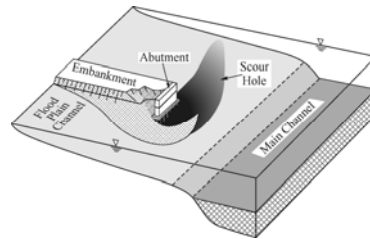
$$Y_{MAX} = \alpha Y_C \quad (3a)$$

in which  $Y_C$  is the mean flow depth at the contraction scour, and  $\alpha$  is an amplification factor

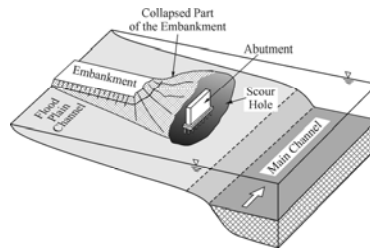
whose value varies in accordance with the distribution of flow contracted through the bridge waterway, and on the characteristics of macro-turbulence structures generated by flow through the waterway (see Fig. 5 for definitions). The value of contraction scour depth  $Y_C$  can be estimated using one of several methods. The method developed by Laursen<sup>2)</sup> is used herein, as it is widely employed.



(a) Scour Condition A



(b) Scour Condition B



(c) Scour Condition C

**Fig. 4** Three abutment-scour conditions considered

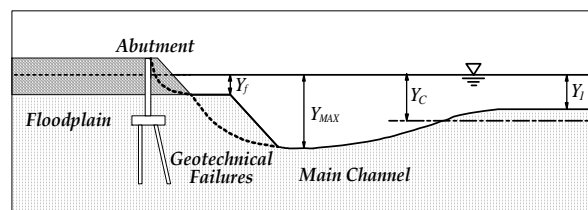


**Fig. 5** Short contraction scour as locally amplified contraction scour (Scour Condition A), and conceptual soil-failure surfaces

Abutment shape, along with the aspects of channel morphology and roughness that affect flow through the bridge waterway, influence amplification coefficient,  $\alpha$ . In developing relationships for estimating the scour depths incurred with Scour Conditions A and B, it is convenient to adapt and extend Laursen's well known methods for estimating live-bed contraction scour<sup>1)</sup>, and for clear-water

scour<sup>3)</sup>.

According to Ettema et al.<sup>4)</sup> the maximum scour depth,  $Y_{MAX}$ , for Scour Condition A is given by

$$Y_{MAX} = \alpha_A Y_C \quad (3b)$$

In terms of the scour depth below the approach-bed level, Eq. (3b) can be re-written as

$$d_{S-MAX} = Y_{MAX} - Y_1 \quad (3c)$$

Similarly, the maximum scour depth,  $Y_{MAX}$ , for Scour Condition B is given by

$$Y_{MAX} = \alpha_B Y_C \quad (3d)$$

And the scour depth below the floodplain bed level is given by

$$d_{S-MAX} = Y_{MAX} - Y_f \quad (3e)$$

Scour of the floodplain at an abutment in Scour Condition C may cause the abutment's embankment slope to become unstable and fail, and eventually to breach. The approach being developed here is basically that used for estimating scour depth at a bridge pier; the exposed abutment is like a pier. Accordingly, one convenient way to relate scour depth to flow is by way of the ratio of approach-flow shear velocity,  $u_*$ , and the critical shear velocity for entrainment of floodplain soil,  $u_{*c}$ ; recall that shear velocity relates to boundary shear stress as  $u_* = \sqrt{\tau / \rho}$ , with  $\tau$  = boundary shear stress and  $\rho$  = water density.

## 4. EXPERIMENTS

### (1) Laboratory experiments

The experimental program entailed five groups of laboratory experiments:

1. Scour at an abutment located on the floodplain (Scour Conditions A and B);
2. Scour at an abutment set back on the floodplain, or located in a rectangular channel, subject to clear-water scour (Scour Condition B);
3. Scour at an exposed abutment column (Scour Condition C);
4. Scour at an abutment with an adjacent pier (Scour Conditions A and B with a pier in close proximity); and,
5. Uncertainties associated with length-scale effects in scour experiments.

### (2) Model channel and model abutments

The laboratory experiments were conducted using a model channel fitted in a sediment re-circulating

flume, 21.3-m long, 4.0-m wide, and 1.0-m deep. The flume accommodated the half width of a compound channel; i.e., the flume width =  $0.5B$ , where  $B$  is the entire width of the compound channel. The width of the floodplain was adjustable, and the floodplain surface could be erodible or fixed. The main channel had a bed of uniform medium sand. The variable erodible natures of floodplain and embankment at bridge sites were simulated by means of tests with the model channel configured in the following arrangements that bracket the variable erodibility of floodplain and embankment:

1. Fixed floodplain and the embankment, both taken to be practically resistant to erosion, whereas the main-channel bed was erodible;
2. Erodeable floodplain and main channel bed (the two being formed of the same noncohesive sediment and equally erodible), with the embankment being erodible but armored with riprap stone; and,
3. Erodeable floodplain and main-channel bed, with the embankment unarmored. The abutment was formed of the same noncohesive sediment as the main-channel bed.

The following prototype considerations and dimensions were used in selecting the model layout, length scale, and dimensions for both types of abutments:

- A road width of 12.0 m (40 ft), in accordance with standard prototype two-lane roads. The road width includes 7.22 m (24 ft) plus 2.7 m (8 ft)-wide shoulders, a total width of 40 ft;
- Pile spacing of 2 m to 3 m (6.6 ft to 9.8 ft);
- Pile diameter of 0.3 m (1 ft);
- The base of the pile cap submerged approximately 1.0 m (3.3 ft) below the original level of the floodplain bed;
- A 2-horizontal:1-vertical (2H:1V) constructed side slope of the earthfill embankment connected to the abutment; and,
- A 2H:1V slope of the bank between the floodplain and the main channel

Considerations of the flume's size led to selection of a geometrically undistorted length scale of 1:30 for the experiments.

The model spill-through abutments were formed around a "standard-stub abutment," which consists of a concrete stub supported by a pile cap on two rows of circular pipes. The design and dimensions of standard-stub abutments commonly used by the Illinois, Iowa, and New York Departments of

Transportation were used in the study (see Fig. 6). Wing-wall abutments usually have similar foundation layout as the standard-stub abutments, as shown in Fig. 7.

A variety of instrumentation devices were used to measure flow velocities and patterns as well as channel bathymetry and scour depth details during the experiments. In particular, an Acoustic Doppler Velocimeter (ADV) was used to determine flow velocities and depths. Large-Scale Particle Image Velocimeter (LSPIV) was employed to obtain two dimensional flow patterns and velocities at the water surface.

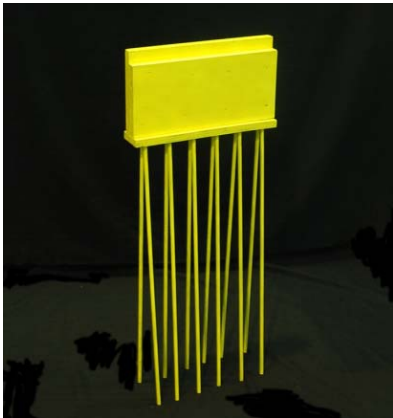


Fig. 6 Model standard-stub column



Fig. 7 Model wing-wall column

## 5. RESULTS FOR SCOUR CONDITION A AT SPILL-THROUGH ABUTMENTS

Definite trends for maximum scour depth were obtained in terms of an overall maximum flow depth,  $Y_{MAX}$ , normalized with long-contraction scour depth,  $Y_C$ , and plotted versus unit-discharge ratio,  $q_2/q_1$ , for the fixed and erodible states of floodplain, which are depicted in Figs. 8 and 9, respectively.

## 6. RESULTS FOR SCOUR CONDITION A AT WING-WALL ABUTMENTS

Laboratory experiments were conducted for fixed wing-wall abutments founded on a fixed floodplain, pile-supported abutments, and abutments supported on sheet-piles. Fig. 10 depicts the primary variables adjusted during the tests. The normalized scour data obtained for the wing-wall abutments located on a fixed floodplain are presented in Fig. 11. As shown in Fig. 9, the largest value of  $Y_{MAX}/Y_C$  for the wingwall abutments is slightly larger than that for the spill-through abutments. The pile-supported and sheet-pile supported wing-wall abutments yielded similar scour trends to those shown in Fig. 11.

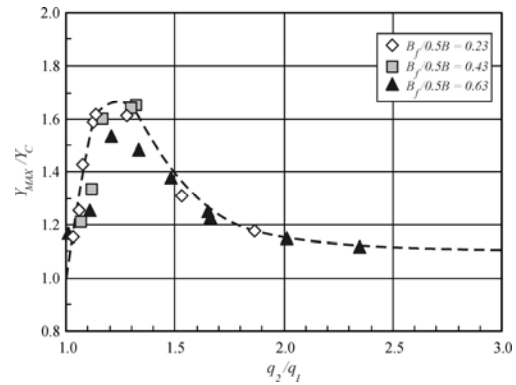


Fig. 8 Variation of  $Y_{MAX}/Y_C$  with  $q_2/q_1$  for Scour Condition A at spill-through abutments on fixed floodplains

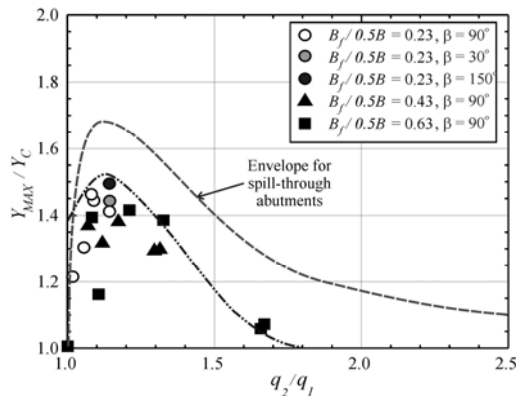


Fig. 9 Variation of  $Y_{MAX}/Y_C$  with  $q_2/q_1$  for Scour Condition A at spill-through abutments on erodible floodplains

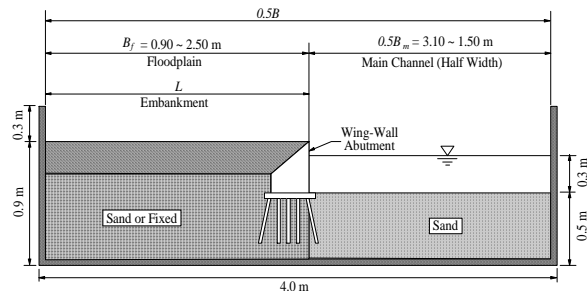


Fig. 10 Principal variables adjusted for wing-wall abutments subject to Scour Condition A

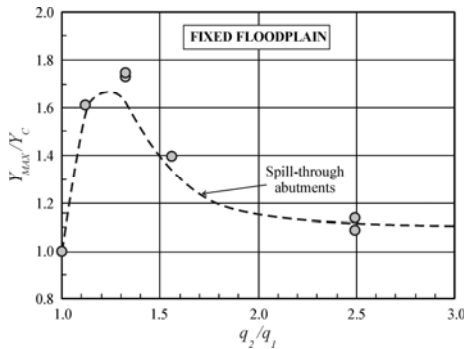


Fig. 11 Variation of  $Y_{MAX}/Y_C$  for wing-wall abutments on fixed floodplains subject to Scour Condition A

## 7. RESULTS FOR SCOUR CONDITION B AT SPILL-THROUGH AND WING-WALL ABUTMENTS

Experimental data obtained under Scour Condition B are presented in Fig. 12 for spill-through and wing-wall abutments in which  $q_{2f}$  denotes the average unit discharge through the bridge waterway at the abutment axis, and  $q_f$  denotes the average unit discharge of flow over the approach floodplain. It is seen in Fig. 12 that  $Y_{MAX}$  substantially exceeds  $Y_C$  at the smaller values of  $q_{2f}/q_f$ , and  $Y_{MAX}/Y_C$  attains a maximum value of about 2.2 when  $q_{2f}/q_f$  is approximately 1.5 for the spill-through abutments and  $Y_{MAX}/Y_C$  is about 2.5 when  $q_{2f}/q_f$  is about 1.1.

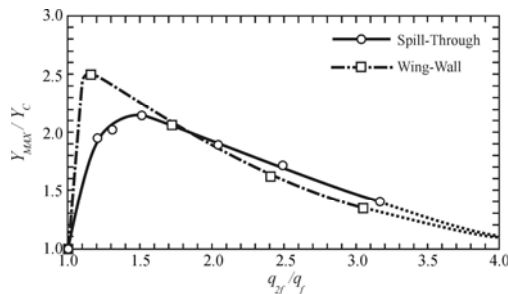


Fig. 12 Variations of flow-depth increase  $Y_{MAX}/Y_C$  against unit-discharge ratio,  $q_{2f}/q_f$ , scour Condition B

## 8. RESULTS FOR SCOUR CONDITION C AT EXPOSED ABUTMENT COLUMNS

Once the embankment was breached, flow around the abutment reduced, and the elevation of the main-channel bed remained more-or-less at its

original level. Scour Condition A usually developed during the earlier stage of scour before the embankment breached. Breaching led to Scour Condition C and the bed level just upstream from the abutment became slightly elevated above its original level. This rise occurred because, once the embankment breached, the approach-flow velocity in the main channel just upstream from the abutment decreased, causing some bed material to deposit.

## 9. CONCLUSIONS

The new design method developed discards the old notion of linearly combining bridge-waterway contraction scour and local scour at the abutment structure, a notion that the laboratory flume experiments do not support. The new method views abutment scour as essentially scour at a short contraction for which the combined influence of nonuniform distribution of flow passing around an abutment, and the generation of large-scale turbulence in flow, passing around an abutment, are intrinsically linked.

Abutment scour may involve three distinct scour conditions, termed Scour Conditions A, B, and C. These scour conditions were observed in the flume experiments and at actual bridge sites.

Furthermore, the geotechnical stability limit for an embankment associated with an abutment was developed, and the scour depth likely to cause embankment failure at the abutment column was evaluated.

**ACKNOWLEDGMENT:** The investigation reported herein was conducted under National Cooperative Highway Research Program (NCHRP) Project 24-20. The authors thank the NCHRP Panel Members for their technical suggestions.

## REFERENCES

- 1) Laursen, E. M.: Scour at bridge crossings, *J. Hydr., Divisions*, ASCE, 86, No. 2, pp. 39-54, 1960.
- 2) Chang, F., and Davis, S.: Maryland Procedure for Estimating Scour at Bridge Abutments, Part 2-Clear Water Scour, *Proc. of Water Resources Engineering*, ASCE, Memphis, TN, pp. 169-173, 1998.
- 3) Laursen, E. M.: An analysis of relief bridge scour, *J. Hydr. Divisions*, ASCE, 86, No. 2, pp. 93-118, 1963.
- 4) Ettema, R., Nakato, T., Yorozuya, A., and Muste, M.: Design estimation of merged localized scour at bridge abutments, *Proc., Int. Conf. on Scour and Erosion, ICSE-3*, Amsterdam, The Netherlands, CD-ROM, 2006.